Damping-Limited Modulation Bandwidths Up to 40 GHz in Undoped Short-Cavity $In_{0.35}Ga_{0.65}As$–GaAs Multiple-Quantum-Well Lasers

S. Weisser, E. C. Larkins, *Member, IEEE*, K. Czotscher, W. Benz, J. Daleiden, I. Esquivias, J. Fleissner,
J. D. Ralston, *Member, IEEE*, B. Romero, R. E. Sah, A. Schönfelder, and J. Rosenzweig

Abstract— We demonstrate record direct modulation bandwidths from MBE-grown $In_{0.35}Ga_{0.65}As$–GaAs multiple-quantum-well lasers with undoped active regions and with the upper and lower cladding layers grown at different growth temperatures. Short-cavity ridge waveguide lasers achieve CW direct modulation bandwidths up to 40 GHz for $6 \times 130~\mu m^2$ devices at a bias current of 155 mA, which is the damping limit for this structure. We further demonstrate large-signal digital modulation up to 20 Gb/s (limited by the measurement setup) and linewidth enhancement factors of 1.4 at the lasing wavelength at threshold of $\sim 1.1~\mu m$ for these devices.

I. Introduction

THE MAXIMUM direct intrinsic modulation bandwidth, $f_{3\,dB}^{max}$, of a semiconductor laser is generally limited by nonlinear gain arising from spectral hole burning, carrier heating or carrier capture/transport processes and is related to the damping-factor (K-factor) by the expression $f_{3\,dB}^{max} = 2\pi\sqrt{2}/K$. Semiconductor lasers with *intrinsic* modulation bandwidths around or exceeding 40 GHz have been demonstrated by several groups, both for GaAs- and InP-based devices. However, the *maximum measured* bandwidths of 26 GHz for InP-based devices [1] and 33 GHz for GaAs-based devices [2] reported to date are substantially lower than the intrinsic modulation bandwidths of these devices. This discrepancy is usually attributed to electrical parasitics, saturation of the relaxation frequency at high bias currents arising from carrier or lattice heating [3], or to lateral multimode behavior. We have recently demonstrated $In_{0.35}Ga_{0.65}As$–GaAs 4 QW lasers with intentionally undoped active regions and *intrinsic* modulation bandwidths of 34

GHz [4]. The *measured* modulation bandwidths were limited to values of 21 GHz ($3 \times 200~\mu m^2$ devices) and 24 GHz ($3 \times 100~\mu m^2$ devices) for lasers fabricated from the epilayer structures reported in [4] and from the improved epilayer structure reported in [5], respectively. In both cases, the modulation bandwidth was limited by saturation of the relaxation frequency at high drive currents and the appearance of higher-order lateral modes. In this work, we present lasers with the same *active layer* design as in [4] and [5], but with further improvements in both the MBE growth parameters and the doping sequence, which achieve the K-factor modulation bandwidth limit of around 40 GHz.

II. Epilayer and Device Structure

The laser structure was grown on 2-in semi-insulating low etch-pit-density horizontal Bridgman GaAs substrates in a Varian GEN II MBE system equipped with an arsenic cracker, a dual-filament Ga effusion cell and a carbon-filament doping source (EPI Systems). The laser structure is comprised of: a 1 μm n^+GaAs ([Si] $= 4 \times 10^{18}$ cm^{-3}) buffer, a lower 0.1 μm n-Al$_x$Ga$_{1-x}$As binary short-period superlattice (SPSL) grading layer ($x = 0 \rightarrow 0.8$ [Si] $= 3 \times 10^{18}$ cm^{-3}), a 0.8 μm lower n-Al$_{0.8}$Ga$_{0.2}$As SPSL cladding layer (0.7 μm [Si] $= 2 \times 10^{18}$ cm^{-3} and 0.1 μm [Si] $= 1 \times 10^{18}$ cm^{-3}), a 28 nm n-Al$_x$Ga$_{1-x}$As SPSL grading layer ($x = 0.8 \rightarrow 0$, [Si] $= 1 \times 10^{18}$ cm^{-3}), 40 nm of undoped GaAs, four 5.7 nm $In_{0.35}Ga_{0.65}As$ QW's separated by 20.1 nm undoped GaAs barriers, 40 nm of undoped GaAs, a 28 nm p-Al$_x$Ga$_{1-x}$As SPSL grading layer ($x = 0 \rightarrow 0.8$, [C] $= 1 \times 10^{18}$ cm^{-3}), a 0.8-μm upper p-Al$_{0.8}$Ga$_{0.2}$As SPSL cladding layer (0.1 μm [C] $= 2 \times 10^{18}$ cm^{-3} and 0.7 μm [Be] $= 2 \times 10^{18}$ cm^{-3}), a 80 nm p-Al$_x$Ga$_{1-x}$As SPSL grading layer ($x = 0.8 \rightarrow 0$ [Be] $= 6 \times 10^{18}$ cm^{-3}), and a 0.2 μm p^{++} contact layer (133 nm [Be] $= 2 \times 10^{19}$ cm^{-3} and 67 nm [Be] $= 8 \times 10^{19}$ cm^{-3}). The p-cladding layers were grown at low growth temperatures (620 °C), reducing the point defect concentration in the active region since the active region is annealed at lower temperatures during the growth of the p-cladding layers. Replacing ternary alloys with SPSL's in the cladding layers further allows the laser structure to be grown at substantially lower growth temperatures [5]. In contrast to [2], [5], where the p- *and* the n-Al$_x$Ga$_{1-x}$As cladding layers were grown at 620 °C, the n-cladding layers in the epilayer structure discussed in this work were grown at their optimum temperature of
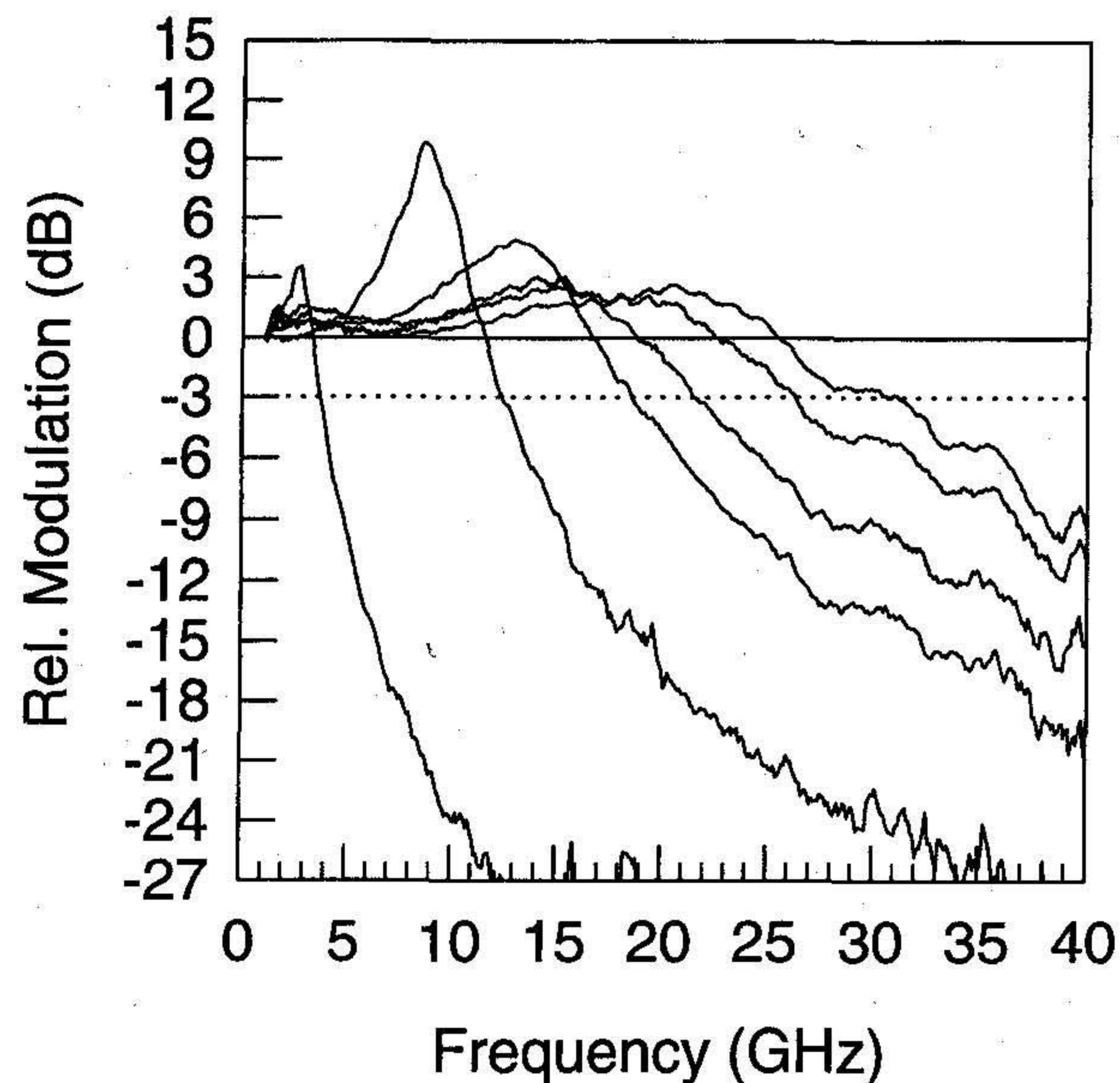
Fig. 1. Small-signal CW modulation response of 6 × 130 μm^2 ridge waveguide laser at various bias currents (10, 20, 40, 60, 80, and 100 mA).
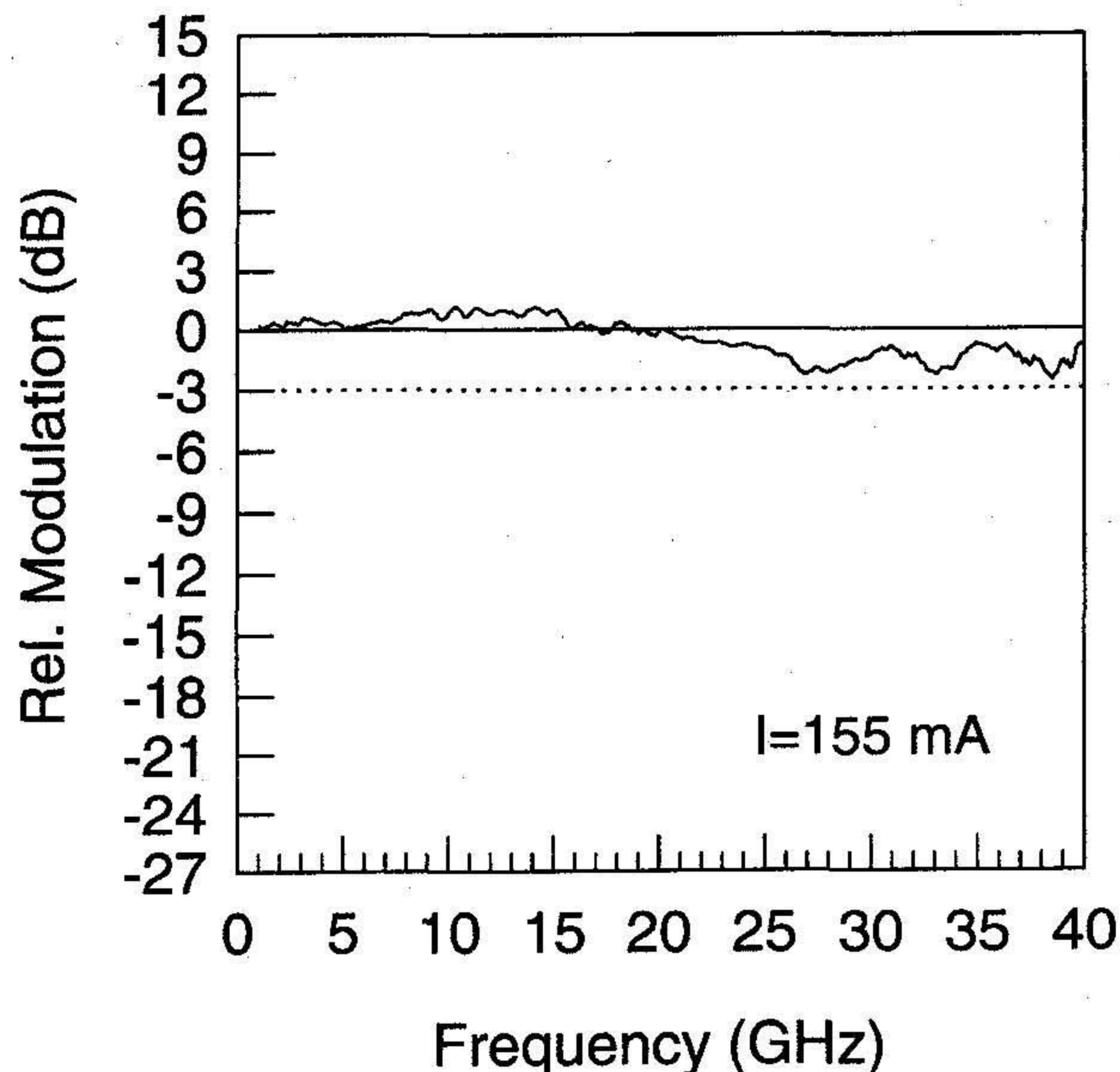

Fig. 2. Small-signal CW modulation response of 6 × 130 μm^2 ridge waveguide laser at a bias current of 155 mA.

Fig. 3. Linewidth enhancement factor versus wavelength of 6 × 130 μm^2 ridge waveguide laser (λ_{th} marks lasing wavelength at threshold).

680–700 °C. Additional modifications include the use of C instead of Be as the dopant in the lower p-cladding layers, preventing p-dopant diffusion into the core during the growth, and increased p- and n-dopant concentrations in the outer cladding layers. Using chemically-assisted ion-beam etching (CAIBE) process for the fabrication of the laser facets, short-cavity ridge waveguide lasers were fabricated in a coplanar triple-mesa geometry suitable for on-wafer probing [6]. Chips containing lasers with one CAIBE-etched and one cleaved facet were indium-soldered epi-side up onto copper/tungsten heat-sinks. The laser facets were not coated.

III. RESULTS AND DISCUSSION

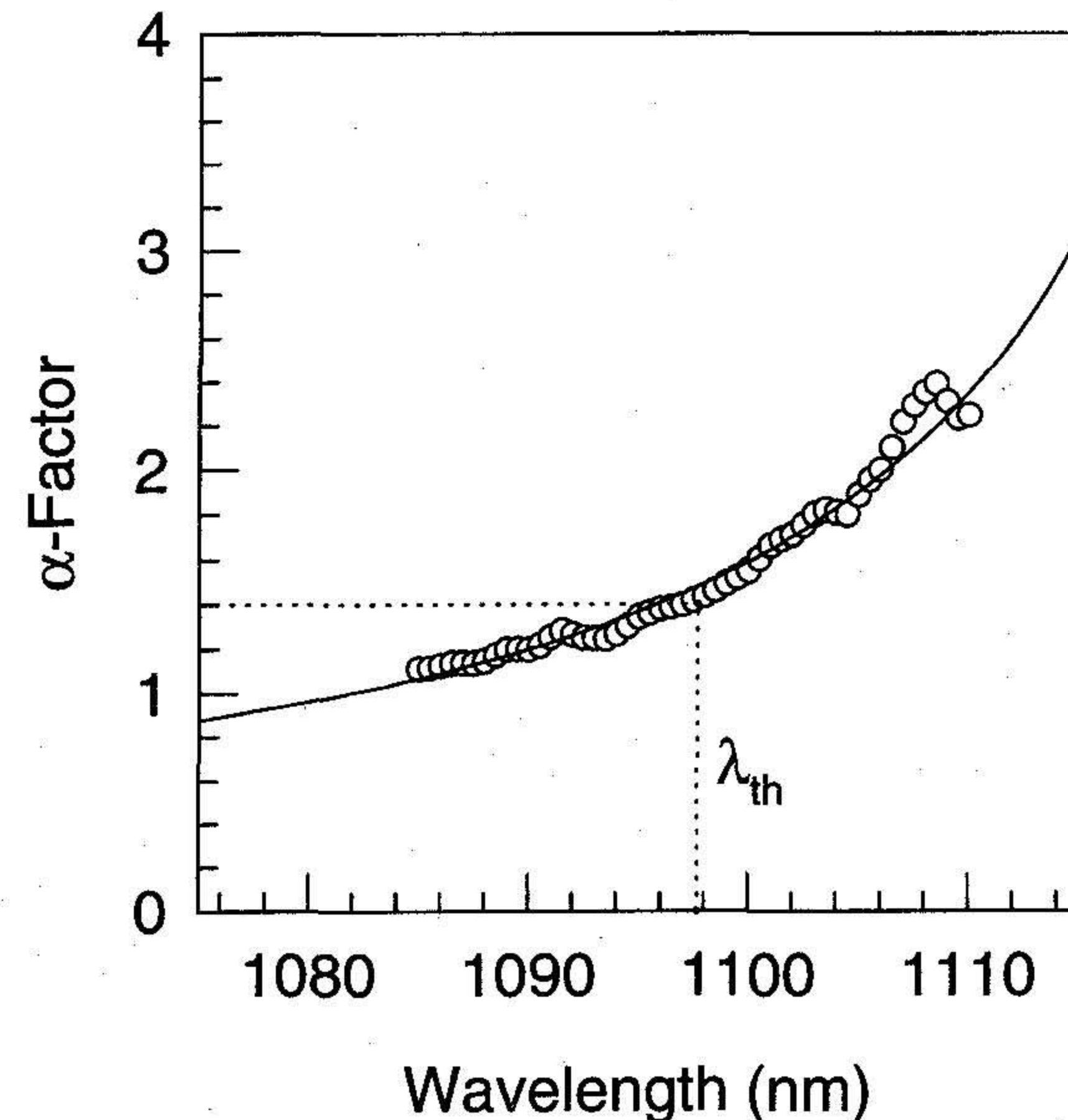All measurements were made at a heat-sink temperature of 25 °C. The average threshold current densities are substantially lower than the corresponding values of the devices reported in [2], [5], with values as low as $J_{th} = 234$ Acm^{-2} for 38 × 500 μm^2 devices. The values of the internal quantum efficiency, η_i, and the internal optical losses, α_i, are 70% and 14 cm^{-1}, respectively. Measurements of the CW optical output power versus drive current show no significant optical power rolloff up to bias currents of $I = 200$ mA (corresponding to a single-facet optical output power of 50 mW) for 6 × 130 μm^2 devices.

The effective carrier lifetime, τ_{eff}, was extracted from values of the frequency-dependent electrical impedance [7] as measured using an HP 8722A network analyzer fully calibrated up to 40 GHz in conjunction with an on-wafer measurement setup. The extracted values of $1/\tau_{eff}^2$ plotted versus the bias current, I, show a linear dependence $1/\tau_{eff}^2 = A^2 + 4$ BI/(qV) [8] (B is the coefficient of radiative recombination, A the linear recombination coefficient, V is the active layer volume, and q is the elementary charge), yielding $A \approx 0$ and $B = 1.3 \times 10^{-10}$ cm^{3}s^{-1} for 6 × 130 μm^2 devices [9]. This result implies that even at low bias currents the effective carrier lifetime is dominated by bimolecular radiative recombination, demonstrating the excellent quality and the low residual doping level in the active region of the optimized epilayer structure discussed in this work.

The modulation response was measured using the same measurement setup in conjunction with a New Focus 1011 photodiode with a 3-dB electrical bandwidth of 45 GHz. Fig. 1 presents typical small-signal modulation response curves of 6 × 130 μm^2 devices (threshold current 8 mA) at various dc bias currents (10–100 mA), revealing modulation bandwidths exceeding 20 GHz and 30 GHz at bias currents of 60 mA and 100 mA, respectively. The relaxation frequency, f_r, and the damping rate, γ, were extracted by fitting the theoretical expression for the modulation response without parasitic contributions and carrier capture/transport effects to the experimentally determined values. The K-factor, extracted
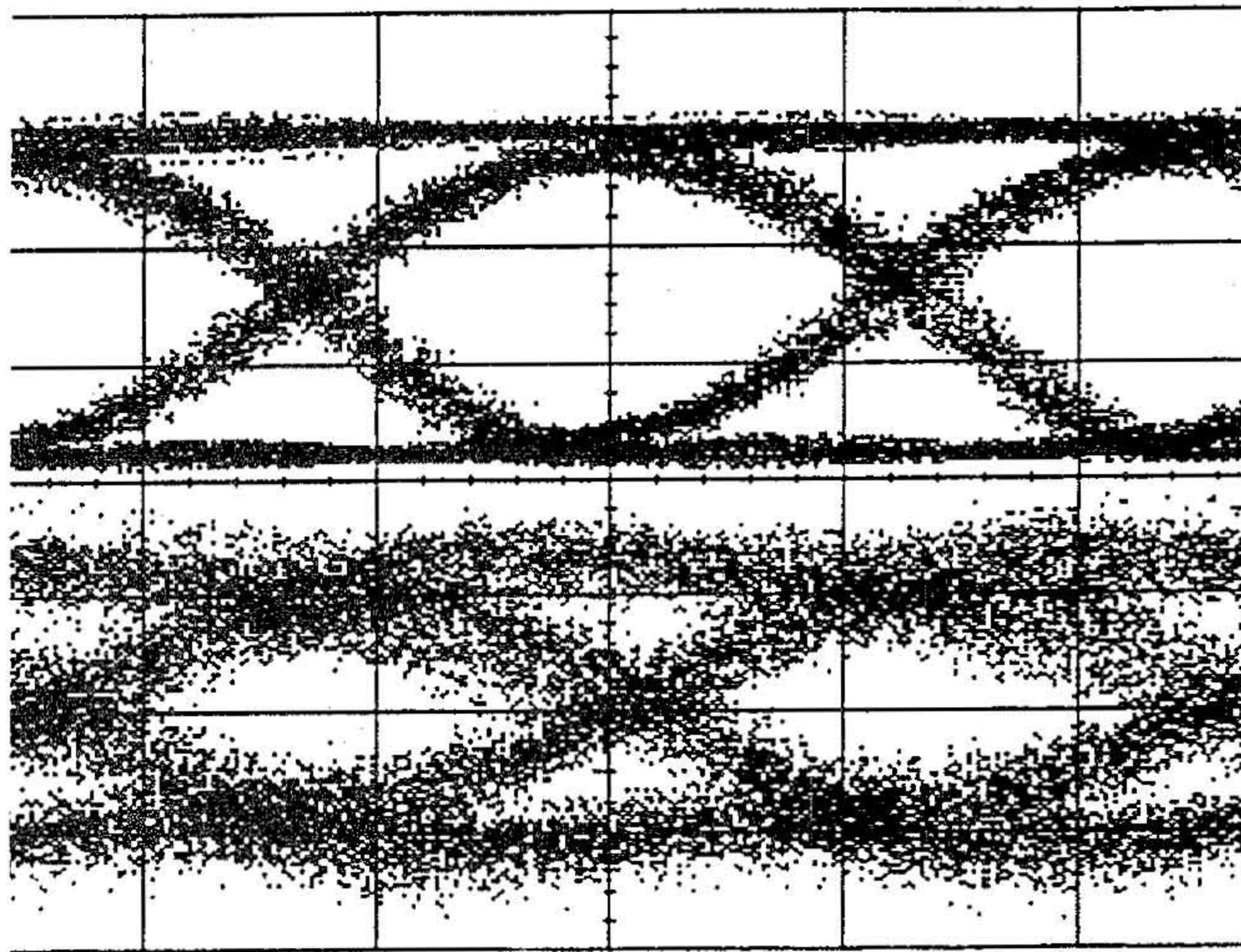
Fig. 4. Eye pattern under 20 Gb/s pseudorandom NRZ modulation of 6 × 130 μm^2 ridge waveguide laser. Upper trace: laser current (bias current 75 mA, peak-to-peak modulation current 50 mA), lower trace: photodiode current (inverted). Time base is 20 ps/div.

from a γ versus f_r^2 plot, is $K = 0.24$ ns at moderate bias currents in good agreement with the corresponding value of 0.27 ns reported in [4]. Fig. 2 presents the modulation response of the best 6 × 130 μm^2 device, revealing a damping-limited 3-dB modulation bandwidth exceeding 40 GHz at a bias current of 155 mA, which is the highest modulation bandwidth reported to date for any semiconductor laser. The fact that the measured maximum bandwidth of around 40 GHz is slightly higher than the value $f_{3\,dB}^{max} = 37$ GHz predicted by the K-factor at low and moderate bias currents is attributed to a slight sublinearity observed in the γ versus f_r^2 characteristics at the highest bias currents [9]. The enhancement in the modulation bandwidth compared to the values reported in [2] is due to the fact that these devices can be operated at substantially higher current densities without saturation of the relaxation frequency ($\sim$20 kAcm^{-2} assuming an active region width of 6 μm in comparison with $\sim$8 kAcm^{-2} for the undoped devices reported in [2]). This superior behavior is attributed to the improved material quality of the optimized epitaxial structure.

The linewidth enhancement factor at threshold, α, was measured using the method described in [10]. Fig. 3 shows the wavelength dependence of α, yielding values as low as $\alpha = 1.4$ at the lasing wavelength at threshold, λ_{th}, of 1097.7 nm. The value of α is substantially lower than the corresponding value for devices fabricated from the nonoptimized structure ($\alpha = 2.3$ [11]).

Large-signal eye diagrams were recorded using an on-wafer measurement setup in conjunction with an Anritsu MP1758A/MP1769A pulse pattern generator. Fig. 4 presents eye diagrams of a 6 × 130 μm^2 laser (bias current 75 mA, peak-to-peak modulation current 50 mA), demonstrating large-signal digital modulation at a data rate of 20 Gb/s. The rise and fall times of the pulses are limited by the detection bandwidth of the HP 54120A/54121A sampling scope (12.5 GHz) and not by the laser dynamics, indicating the suitability of these devices for large-signal digital modulation at data rates beyond 20 Gb/s.

IV. CONCLUSION

We have fabricated short-cavity In$_{0.35}$Ga$_{0.65}$As–GaAs MQW lasers with undoped active regions using an epilayer structure grown under carefully tailored MBE growth conditions in conjunction with optimized doping sequences in the cladding layers. The best 6 × 130 μm^2 devices have attained a damping-limited 3-dB modulation bandwidth up to 40 GHz at a dc bias current of 155 mA. The devices further demonstrate linewidth enhancement factors of $\alpha = 1.4$ and are suitable for large-signal digital modulation at data rates of at least 20 Gb/s.

REFERENCES

[1] P. A. Morton, T. Tanbun-Ek, R. A. Logan, N. Chand, K. W. Wecht, A. M. Sergent, and P. F. Sciortino, Jr., "Packaged 1.55 μm DFB laser with 25 GHz modulation bandwidth," *Electron. Lett.*, vol. 30, pp. 2044–2046, 1994.

[2] J. D. Ralston, S. Weisser, K. Eisele, R. E. Sah, E. C. Larkins, J. Rosenzweig, J. Fleissner, and K. Bender, "Low-bias-current direct modulation up to 33 GHz in InGaAs/GaAs/AlGaAs pseudomorphic MQW ridge-waveguide lasers," *IEEE Photon. Technol. Lett.*, vol. 6, pp. 1076–1079, 1994.

[3] R. M. Spencer, S. S. O' Keefe, W. J. Schaff, L. F. Eastman, and C.-Y. Tsai, "Temperature effects on the high speed performance of quantum well lasers," in *Proc. IEEE Lasers and Electro-Opt. Soc. '95 Annu. Meet.*, 1995, vol. 1, pp. 99–100.

[4] J. D. Ralston, S. Weisser, I. Esquivias, E. C. Larkins, J. Rosenzweig, P. J. Tasker, and J. Fleissner, "Control of differential gain, nonlinear gain, and damping factor for high-speed application of GaAs-based MQW lasers," *IEEE J. Quantum Electron.*, vol. 29, pp. 1648–1659, 1993.

[5] E. C. Larkins, W. Benz, I. Esquivias, W. Rothemund, M. Baeumler, S. Weisser, A. Schönfelder, J. Fleissner, W. Jantz, J. Rosenzweig, and J. D. Ralston, "Improved performance from pseudomorphic In$_y$Ga$_{1-y}$As/GaAs MQW lasers with low growth temperature Al$_x$Ga$_{1-x}$As short-period superlattice cladding," *IEEE Photon. Technol. Lett.*, vol. 7, pp. 16–19, 1995.

[6] S. D. Offsey, W. J. Schaff, P. J. Tasker, and L. F. Eastman, "Optical and microwave performance of GaAs–AlGaAs and strained layer InGaAs–GaAs–AlGaAs graded index separate confinement heterostructure single quantum well lasers," *IEEE Photon. Technol. Lett.*, vol. 2, pp. 9–11, 1990.

[7] S. Weisser, I. Esquivias, P. J. Tasker, J. D. Ralston, B. Romero, and J. Rosenzweig, "Impedance characteristics of quantum-well lasers," *IEEE Photon. Technol. Lett.*, vol. 6, pp. 1421–1424, 1994.

[8] R. Olshansky, C. B. Su, J. Manning, and W. Powazinik, "Measurement of radiative and nonradiative recombination rates in InGaAsP and AlGaAs light sources," *IEEE J. Quantum Electron.*, vol. QE-20, pp. 838–854, 1984.

[9] S. Weisser, E. C. Larkins, K. Czotscher, W. Benz, J. Daleiden, I. Esquivias, J. Fleissner, M. Maier, J. D. Ralston, B. Romero, R. E. Sah, A. Schönfelder, and J. Rosenzweig, "CW direct modulation bandwidths up to 40 GHz in short-cavity In$_{0.35}$Ga$_{0.65}$As/GaAs MQW lasers with undoped active regions," in *Proc. '95 Europ. Conf. Optical Commun. (ECOC)*, 1995, pp. 1015–1018.

[10] B. Zhao, T. R. Chen, S. Wu, Y. H. Zhuan, Y. Yamada, and A. Yariv, "Direct measurement of linewidth enhancement factors in quantum well lasers of different quantum well barrier heights," *Appl. Phys. Lett.*, vol. 62, pp. 1591–1593, 1993.

[11] A. Schönfelder, S. Weisser, J. D. Ralston, and J. Rosenzweig, "Differential gain, refractive index, and linewidth enhancement factor in high-speed GaAs-based MQW lasers: Influence of strain and p-doping," *IEEE Photon. Technol. Lett.*, vol. 6, pp. 891–893, 1994.